Theory of the vibrational structure of resonances in electron-molecule scattering

W. Domcke and L. S. Cederbaum
Fakultät für Physik der Universität Freiburg, D-78 Freiburg, Germany
(Received 27 December 1976)

We derive a simple Hamiltonian representing the coupling of an electronic level of positive energy to the continuum of scattering states as well as to the molecular vibrations. By summing the perturbation series for the S matrix to infinite order in the bound-state–continuum interaction, an effective non-Hermitian boson Hamiltonian describing the dynamics of vibrational motion in the resonance state is obtained. It is shown that the effective Hamiltonian can be diagonalized, yielding explicit expressions for the vibrational excitation cross sections. The theory is applied to two representative examples, the 3.8-eV shape resonance in CO_2 and the 2.4-eV shape resonance in N_2. The results exhibit a clear improvement over those obtained with existing theories, which express the cross sections in terms of conventional Franck-Condon factors. The influence of the anharmonicity of the potential functions on the structure of the vibrational excitation functions is discussed.

I. INTRODUCTION

The occurrence of resonances in the scattering of electrons from atoms and molecules is a well-known phenomenon.[1,2] The vibrational excitation of molecules by low-energy electrons proceeds most effectively via resonant processes. While resonances in diatomic molecules have been extensively investigated for a long time,[2] most of the recent experimental work concentrates on polyatomic molecules.[3-8]

It has been found that a variety of resonances is usually associated with a given molecule. The resonances can be classified according to the molecular parent state from which they derive by the attachment of an electron.[2,9,10] In the context of vibrational excitation, a classification of the resonances according to the ratio Γ/ω, where Γ is the resonance width, and ω the vibrational frequency, has been found useful.[9,11,12] In the limit $\Gamma \ll \omega$, which has been termed the compound-molecule limit,[9] the cross sections in the elastic and the vibrationally inelastic channels exhibit narrow peaks corresponding to the vibrational levels of the temporary negative ion. The resonance thus decomposes into a number of vibrational subresonances, similar to the spreading of the oscillator strength of an electronic transition over a number of vibrational levels according to the Franck-Condon principle.[13] In the opposite limit, $\Gamma \gg \omega$, usually called the impulse limit,[9] there are no well-defined vibrational levels of the negative ion. Correspondingly, the various vibrational cross sections exhibit a broad and structureless hump. The intermediate case $\Gamma \approx \omega$ has been found to be of particular interest.[12,14] The prototype example is the 2.4 eV shape resonance in N_2.[2] The vibrational cross sections exhibit an oscillatory structure which changes in a peculiar manner as the vibrational quantum number of the final state increases. The maxima and minima shift towards higher energy and the separation and the width of the peaks increase markedly. Recently, the 3.8-eV shape resonance in CO_2 has been found to exhibit this behavior in an even more pronounced form.[15,16]

We confine ourselves in the present work to the discussion of the vibrational phenomena in resonant electron-molecule scattering. We shall not be concerned with the calculation of absolute cross sections, angular distributions, and rotational excitation. Methods to calculate absolute-scattering cross sections for small molecules have been developed and applied by Temkin and Vasavada,[17] Henry and Lane,[18] Burke *et al.*,[19] Schneider,[20] Morrison *et al.*,[21] Rescigno *et al.*,[22] and Chandra and Temkin.[23] Cross sections for simultaneous excitation of vibration and rotation as well as angular distributions have been calculated by the latter authors, and by Henry[24] and Brandt *et al.*[25] While the rotational structure of the scattering cross section cannot be resolved in present experiments and the determination of total cross sections is difficult,[2] the vibrational structure of the elastic and vibrationally inelastic cross sections is easily observable and of considerable current interest. In view of recent experimental work on larger molecules such as formaldehyde[6] or benzene,[4] a theoretical approach which is general and simple enough to be applicable to such complex systems is of interest.

II. CALCULATION OF VIBRATIONAL-EXCITATION CROSS SECTIONS

Instead of starting from the full scattering wave function and the associated Schrödinger equation and introducing approximations to the wave func-

tion, our approach is to formulate a model Hamiltonian which describes only those processes we are interested in and which is simple enough to be amenable to an exact solution.

A. Hamiltonian

As is well known, resonances are—from the conceptual as well as from the computational point of view—best described as bound states embedded in the continuum. The mathematical formulation of this idea is due to Feshbach[26] and Fano.[27] The approach of Feshbach is to introduce two projection operators P and Q

$$P+Q=1, \quad P^2=P, \quad Q^2=Q$$

with the requirement

$$P\Psi \xrightarrow[|\vec{r}|\to\infty]{} \Psi ,$$

where Ψ is the total scattering wave function and $\vec{r}$ refers to the position of the scattered electron. $P\Psi$ thus exhibits the correct asymptotic behavior while $Q\Psi$ vanishes asymptotically. The full Hamiltonian of the system is now decomposed according to

$$H=(P+Q)H(P+Q)=H_{QQ}+H_{PP}+H_{PQ}+H_{QP}, \quad (1)$$

where H_{QQ} stands for QHQ, etc. Q can be chosen such that the eigenvalues of H_{QQ} are discrete,[28] while H_{PP} has a continuous spectrum. H_{PQ} and H_{QP} represent the coupling of the discrete states to the continuum.

Guided by these ideas, we now formulate a Hamiltonian which is suitable for the description of the vibrational phenomena in the resonant scattering of electrons from molecules. To describe the electronic motion for a fixed nuclear configuration characterized by a set of M internal coordinates $\vec{R}$, the field operator[29,30] $\psi(\vec{r})$, which annihilates an electron at the position $\vec{r}$, is expanded in terms of a suitable basis set of one-particle functions,

$$\psi(\vec{r})=\sum_i \varphi_i(\vec{r},\vec{R})a_i+\sum_k \varphi_k(\vec{r},\vec{R})a_k$$
$$\equiv \psi_Q(\vec{r})+\psi_P(\vec{r}) , \quad (2)$$

where a_i and a_k are the annihilation operators[29,30] for a particle in the orbital $\varphi_i(\vec{r},\vec{R})$ and $\varphi_k(\vec{r},\vec{R})$, respectively. The $\varphi_i(\vec{r},\vec{R})$ are square-integrable one-particle wave functions corresponding to discrete one-particle states and the $\varphi_k(\vec{r},\vec{R})$ are continuum one-particle wave functions. The continuum states $|\varphi_k\rangle$ are chosen to form an orthonormal set orthogonal to the bound one-particle states $|\varphi_i\rangle$

$$\langle\varphi_k|\varphi_{k'}\rangle=\delta(k-k') , \quad \langle\varphi_i|\varphi_k\rangle=0 . \quad (3)$$

Restricting ourselves, for the moment, to the one-particle approximation, the electronic Hamiltonian takes the form

$$H^{el}=\int d^3r\,\psi^\dagger(\vec{r})H^{el}(\vec{r},\vec{R})\psi(\vec{r}) ,$$
$$\equiv H^{el}_{QQ}+H^{el}_{PP}+H^{el}_{PQ}+H^{el}_{QP} , \quad (4)$$

where

$$H^{el}_{QQ}=\int d^3r\,\psi^\dagger_Q(\vec{r})H^{el}(\vec{r},\vec{R})\psi_Q(\vec{r})$$
$$=\sum_i \epsilon^0_i(\vec{R})a^\dagger_i a_i ,$$
$$H^{el}_{PP}=\int d^3r\,\psi^\dagger_P(\vec{r})H^{el}(\vec{r},\vec{R})\psi_P(\vec{r})$$
$$=\sum_k \epsilon_k a^\dagger_k a_k+\sum_{k'\neq k} V_{kk'}a^\dagger_k a_{k'} ,$$
$$H^{el}_{PQ}=\int d^3r\,\psi^\dagger_P(\vec{r})H^{el}(\vec{r},\vec{R})\psi_Q(\vec{r})$$
$$=\sum_{k,i} V_{ki}(\vec{R})a^\dagger_k a_i ,$$

and the ϵ^0_i, ϵ_k, $V_{kk'}$, and V_{ik} are the corresponding matrix elements of $H^{el}(\vec{r},\vec{R})$, i.e.,

$$\epsilon^0_i(\vec{R})=\int d^3r\,\varphi^*_i(\vec{r},\vec{R})H^{el}(\vec{r},\vec{R})\varphi_i(\vec{r},\vec{R}) ,$$

etc. The bound state orbitals φ_i have been assumed to diagonalize H_{QQ}. Since the continuum orbitals φ_k are subject to the condition (3), they cannot be freely chosen to diagonalize H_{PP}. In addition, it is assumed that ϵ_k and $V_{kk'}$ are independent of the nuclear coordinates $\vec{R}$.

To include the vibrational degrees of freedom we have to augment this Hamiltonian by the nuclear kinetic-energy operator and the electrostatic repulsion energy of the nuclei. Expanding this latter energy and the orbital energies $\epsilon^0_i(\vec{R})$ in powers of $\vec{R}-\vec{R}_0$, where $\vec{R}_0$ is the equilibrium geometry of the molecule in the electronic ground state, we obtain in the harmonic approximation for the closed channel part of the Hamiltonian[31-33]

$$H_{QQ}=\sum_i \epsilon^0_i(0)a^\dagger_i a_i+\sum_{s=1}^{M}\omega_s(b^\dagger_s b_s+\tfrac{1}{2})$$
$$+\sum_i\sum_{s=1}\kappa^0_{i,s}(a^\dagger_i a_i-n_i)(b_s+b^\dagger_s)$$
$$+\sum_i\sum_{s_1 s'=1}^{M}\gamma^0_{i,ss'}(a^\dagger_i a_i-n_i)(b_s+b^\dagger_s)(b_{s'}+b^\dagger_{s'}) , \quad (5)$$

where n_i is the occupation number of the orbital i, i.e.,

$n_i = 1(0)$ for orbitals occupied (unoccupied) in the electronic ground state. The b_s and $b_s^\dagger$ are annihilation and creation operators for vibrational quanta[29] and related to the (dimensionless) normal coordinates Q_s[34] of the molecule in its electronic ground state according to

$$b_s = 2^{-1/2}(Q_s + \partial/\partial Q_s), \quad b_s^\dagger = 2^{-1/2}(Q_s - \partial/\partial Q_s).$$

The set of dimensionless normal coordinates $\vec{Q}$ is connected with the set of internal coordinates $\vec{R} - \vec{R}_0$ by the usual linear transformation $\underline{L}$[34]

$$\vec{R} - \vec{R}_0 = \underline{L}\underline{\omega}^{-1/2}\vec{Q}, \tag{6}$$

where $\underline{\omega}$ denotes the diagonal matrix of ground state vibrational frequencies $\omega_s, s = 1 \ldots M$. The $\kappa^0_{i,s}$ and $\gamma^0_{i,ss'}$ are the linear and quadratic coupling constants[32] describing the interaction between the electronic and vibrational motion and are given by

$$\kappa^0_{i,s} = \frac{1}{\sqrt{2}}\left(\frac{\partial \epsilon_i^0}{\partial Q_s}\right)_0, \quad \gamma^0_{i,ss'} = \frac{1}{4}\left(\frac{\partial^2 \epsilon_i^0}{\partial Q_s \partial Q_{s'}}\right)_0 . \tag{7}$$

The subscript 0 indicates that the derivative is to be evaluated at the equilibrium geometry of the electronic ground state.

Some remarks on the Hamiltonian (5) are appropriate. Firstly, it must be admitted that the harmonic approximation may be a poor or even inappropriate one in some cases. However, the restriction to the harmonic approximation is indispensable to render the problem solvable in a closed and transparent form. The influence of anharmonic effects will be discussed in some detail in Sec. IIIB. Secondly, we shall adopt the adiabatic approximation.[35] It consists in the assumption that the electronic operators a_i, $a_i^\dagger$ commute with the boson operators b_s, $b_s^\dagger$, although they depend on the nuclear coordinates, as can be seen from Eq. (2). In the usual phraseology, the a_i, $a_i^\dagger$ are assumed to depend "only parametrically" on the nuclear coordinates.[33] Finally, it is important to note that using the Hamiltonian (5) we are by no means tied to the one-particle picture introduced for the derivation of Eq. (5). In the adiabatic approximation and provided that a quasiparticle picture[30] is applicable, the ϵ_i^0, $\kappa^0_{i,s}$ and $\gamma^0_{i,ss'}$ can be "renormalized" to include reorganization and correlation effects.[31,32] The linear and quadratic vibrational coupling constants are still given by Eq. (7), but with the one-particle energy $\epsilon_i^0(\vec{Q})$ replaced by the corresponding renormalized level energy. Thus, all previously developed bound state methods for calculating resonance energies[36-40] can be used to obtain the renormalized $\epsilon_i^0(0)$ and the renormalized coupling constants $\kappa^0_{i,s}$ and $\gamma^0_{i,ss'}$.

For the ensuing calculation we rewrite our final Hamiltonian, (4) and (5), in the form

$$H = H_0 + H_1,$$

$$H_0 = \sum_i \epsilon_i^0(0) a_i^\dagger a_i + \sum_k \epsilon_k a_k^\dagger a_k + \sum_{s=1}^{M} \omega_s (b_s^\dagger b_s + \tfrac{1}{2}) + \sum_i \sum_{s=1}^{M} \kappa^0_{i,s}(a_i^\dagger a_i - n_i)(b_s + b_s^\dagger) + \sum_i \sum_{s,s'=1}^{M} \gamma^0_{i,ss'}(a_i^\dagger a_i - n_i)(b_s + b_s^\dagger)(b_{s'} + b_{s'}^\dagger), \tag{8a}$$

$$H_1 = \sum_{i,k} (V_{ik} a_i^\dagger a_k + V_{ki} a_k^\dagger a_i) + \sum_{k,k'} V_{kk'} a_k^\dagger a_{k'} . \tag{8b}$$

The first term in H_1, which causes electrons to "hop" between the one-particle states $|\varphi_i\rangle$ and $|\varphi_k\rangle$ and thus converts the closed-channel states $|\varphi_i\rangle$ into resonances, is analogous to the hopping interaction in the well-known Anderson Hamiltonian,[41] widely used to describe magnetic impurity centers in metals[42] and atoms chemisorbed on metal surfaces.[43] As noted above, the ϵ_k and the direct scattering potential $V_{kk'}$ are assumed to be independent of the nuclear coordinates $\vec{Q}$, which means that electrons in the continuum states $|\varphi_k\rangle$ do not couple to the molecular vibrations. We are thus neglecting direct vibrational excitation through the dipole and polarization mechanisms.[37,44] The direct vibrational excitation is usually weak compared to the vibrational excitation via resonances. Finally, it should be noted that the matrix elements V_{ik} are in general functions of the nuclear coordinates $\vec{Q}$, and thus, do not commute with the boson operators b_s, $b_s^\dagger$.

B. Transition probability and cross sections

For definiteness, we consider shape resonances[2,9] associated with the electronic ground state of the target molecule. The incident electron is captured temporarily in the field of the target molecule; after its reemission, the molecule is left in its electronic ground state, but possibly vibrationally excited. The asymptotic initial and final states are then

$$|I,p\rangle = a_p^\dagger |\Psi_I^N\rangle, \quad |F,p'\rangle = a_{p'}^\dagger |\Psi_F^N\rangle , \tag{9}$$

where $|\Psi_I^N\rangle$ is the ground-state wave function of the target with N electrons. In the adiabatic approximation[35]

$$|\Psi_I^N\rangle = |\varphi_0^N\rangle |\vec{0}\rangle . \tag{10}$$

Correspondingly, the target state vector after the interaction is

$$|\Psi_F^N\rangle = |\varphi_0^N\rangle |n_1 \ldots n_M\rangle . \tag{11}$$

$|\varphi_0^N\rangle$ denotes the ground state of the N-electron system, $|\vec{0}\rangle$ the vibrational ground state of the target molecule and $|n_1 \ldots n_M\rangle$ a vibrationally excited state with n_s quanta of the sth normal mode excited. The corresponding initial and final-state energies are

$$E_I = E_0^N + \sum_{s=1}^{M} \tfrac{1}{2}\omega_s + \epsilon_p \,, \qquad E_F = E_0^N + \sum_{s=1}^{M} \omega_s(n_s + \tfrac{1}{2}) + \epsilon_{p'} \,, \tag{12}$$

E_0^N denoting the electronic-ground-state energy. With these definitions, the total transition probability from the initial to the final state is given by[45]

$$W_{p'p}(n_1, \ldots, n_M) = \lim_{\tau\to\infty} (1/\tau)\, |\langle F, p' | S(\tau) | I, p\rangle|^2 \tag{13}$$

with the S matrix

$$S(\tau) = \mathcal{T} \exp\left(-i \int_{-\infty}^{\tau} dt\, H_1(t)\right) , \tag{14}$$

$$H_1(t) = e^{iH_0 t} H_1 e^{-iH_0 t} , \tag{15}$$

where $\mathcal{T}$ is the Dyson time-ordering operator.[46] Introducing the T matrix

$$\lim_{\tau\to\infty} \langle F, p' | S(\tau) | I, p\rangle = -2\pi i \delta(E_F - E_I) \langle F, p' | T | I, p\rangle \,, \tag{16}$$

we have for the transition probability per unit time[45]

$$w_{p'p}(n_1, \ldots, n_M) = 2\pi\delta\left(\epsilon_{p'} - \epsilon_p + \sum_{s=1}^{M} n_s \omega_s\right) |\langle F, p' | T | I, p\rangle|^2 . \tag{17}$$

Since shape resonances in actual molecules are usually well separated and do not interact appreciably with one another, it is sufficient to consider only one resonance orbital i. In addition, we restrict ourselves to pure resonance scattering, i.e., we neglect the direct scattering term in H_1 [the second term in Eq. (8b)]. Expanding now the S matrix in a perturbation series in H_1

$$S(\tau) = 1 - i \int_{-\infty}^{\tau} dt\, H_1(t) - \int_{-\infty}^{\tau} dt \int_{-\infty}^{t} dt'\, H_1(t) H_1(t') + \cdots , \tag{18}$$

it is clear that the lowest term giving a nonvanishing contribution is of second order in H_1. The corresponding lowest-order expression for the transition probability per unit time is

$$w_{p'p}^{(4)}(n_1, \ldots, n_M) = 2\pi\delta\left(\epsilon_{p'} - \epsilon_p + \sum_{s=1}^{M} n_s \omega_s\right) |\langle F, p' | T^{(2)} | I, p\rangle|^2 ,$$

$$\langle F, p' | T^{(2)} | I, p\rangle = \langle F, p' | H_1 (E_I - H_0 + i\eta)^{-1} H_1 | I, p\rangle \,, \tag{19}$$

where η is a positive infinitesimal. Using the explicit form of the states $|I, p\rangle$ and $|F, p'\rangle$ given in Eqs. (9)–(11) and the commutation relations for the electronic creation and annihilation operators,[29] we obtain in the adiabatic approximation

$$\langle F, p' | T^{(2)} | I, p\rangle = \langle n_1 \ldots n_M | V_{p'i} \times (\epsilon_p - \tilde{H} + i\eta)^{-1} V_{ip} | \vec{0}\rangle \,, \tag{20}$$

where $\tilde{H}$ is a pure boson Hamiltonian,

$$\tilde{H} = \epsilon_i^0(0) + \sum_{s=1}^{M} \omega_s b_s^\dagger b_s + \sum_{s=1}^{M} \kappa_{i,s}^0 (b_s + b_s^\dagger) + \sum_{s,s'=1}^{M} \gamma_{i,ss'}^0 (b_s + b_s^\dagger)(b_{s'} + b_{s'}^\dagger) . \tag{21}$$

The physical meaning of these expressions is the following. The δ function in Eq. (19) describes the energy conservation in the scattering process, while the square of the matrix element (20) governs the distribution of the intensity over the final vibrational states. The Hamiltonian $\tilde{H}$ describes the vibrational motion in the intermediate (resonance) state. However, there appears no width associated with the resonance state in the above lowest-order expressions: $\tilde{H}$ of Eq. (21) describes vibrational motion in a stationary electronic state. Eqs. (19) to (21) are thus not capable of giving an adequate description of resonance phenomena.

Obviously, we have to include higher-order terms in the perturbation expansion of the S matrix. The series for the S matrix (or, equivalently, the T matrix) can indeed be summed exactly within the approximations introduced above. The T matrix satisfies the equation[45]

$$T = H_1 + H_1 (E_I - H_0 + i\eta)^{-1} T = H_1 + H_1 (E_I - H_0 + i\eta)^{-1} H_1 + \cdots . \tag{22}$$

Only the terms containing even powers of H_1 contribute to the resonance scattering. Considering, for example, the term of fourth order in H_1, we obtain within the adiabatic approximation

$$\langle F, p' | T^{(4)} | I, p\rangle = \langle n_1 \ldots n_M | V_{p'i} (\epsilon_p - \tilde{H} + i\eta)^{-1} \times \left(\sum_k V_{ik} (\epsilon_p - \epsilon_k - \tilde{H}_0 + i\eta)^{-1} V_{ki}\right) \times (\epsilon_p - \tilde{H} + i\eta)^{-1} V_{ip} | \vec{0}\rangle \tag{23}$$

with $\tilde{H}$ given by Eq. (21) and

$$\tilde{H}_0 = \sum_{s=1}^{M} \omega_s b_s^\dagger b_s \,. \tag{24}$$

The series represented by Eqs. (20) and (23) and the higher-order terms can now be summed *exactly*, giving

$$\langle F, p' \,|\, T \,|\, I, p\rangle$$
$$= \Big\langle n_1 \ldots n_M \,\Big|\, V_{p'i}$$
$$\times \Big(\epsilon_p - \tilde{H} - \sum_k V_{ik}(\epsilon_p - \epsilon_k - \tilde{H}_0 + i\eta)^{-1} V_{ki}\Big)^{-1} V_{ip} \,\Big|\, \vec{0}\Big\rangle . \tag{25}$$

Rewriting this equation in a more compact form we arrive at our final result

$$\langle F, p' \,|\, T \,|\, I, p\rangle = \langle n_1 \ldots n_M \,|\, V_{p'i}(\epsilon_p - \mathcal{H})^{-1} V_{ip} \,|\, \vec{0}\rangle \tag{26}$$

with

$$\mathcal{H} = \tilde{H} + \Delta_i - \tfrac{1}{2} i \Gamma_i \,, \tag{27}$$

$$\Delta_i = P \sum_k V_{ik} \frac{1}{\epsilon_p - \epsilon_k - \tilde{H}_0} V_{ki} \,, \tag{28}$$

$$\Gamma_i = 2\pi \sum_k V_{ik} \delta(\epsilon_p - \epsilon_k - \tilde{H}_0) V_{ki} \,. \tag{29}$$

The difference between Eq. (26) and the lowest-order approximation, Eq. (20), is evident. The resonance has now received a width, given by Eq. (29), and has been shifted by an amount Δ_i, Eq. (28). The vibrational motion in the intermediate state is now described by the non-Hermitian Hamiltonian $\mathcal{H}$.

The vibrational excitation cross section is, apart from kinematic factors,[45] given by

$$\frac{d\sigma_{n_1 \ldots n_M}}{d\Omega} \sim (|p'|/|p|)\, |\langle F, p' \,|\, T \,|\, I, p\rangle|^2$$
$$= (|p'|/|p|)\, |\langle n_1 \ldots n_M \,|$$
$$\times V_{p'i} (\epsilon_p - \mathcal{H})^{-1} V_{ip} \,|\, \vec{0}\rangle \,|^2 . \tag{30}$$

Note that the intermediate state vibrational Hamiltonian $\mathcal{H}$ is of a rather complicated nature, since Δ_i and Γ_i are not simply functions of the nuclear coordinates $\vec{Q}$ (due to the $\vec{Q}$-dependence of V_{ik}), but are operators in $\vec{Q}$ space. To a first approximation, however, one may omit the operator $\tilde{H}_0$ in Eqs. (28), and (29) and consider Δ_i and Γ_i as functions of $\vec{Q}$. Neglecting further the energy dependence of Δ_i and Γ_i, the Hamiltonian $\mathcal{H}$ describes the vibrational motion in a complex adiabatic potential. The concept of vibrational motion in a complex adiabatic potential has first been used by Bardsley, Herzenberg, and Mandl[47] to calculate vibrational-excitation cross sections. Our expressions Eqs. (28) and (29) for Δ_i and Γ_i contain nonadiabatic corrections to this approximation.

In what follows we neglect these nonadiabaticities and the energy dependence of Δ_i and Γ_i and retain only their $\vec{Q}$ dependence. As first shown by Birtwistle and Herzenberg,[14] the consideration of the $\vec{Q}$ dependence of Γ_i is essential for an understanding of the structure of the cross sections. Expanding Δ_i and Γ_i about the equilibrium geometry of the molecule in its ground state up to second order in the normal coordinates Q_s, $\mathcal{H}$ takes the form

$$\mathcal{H} = \epsilon_i + \sum_{s=1}^{M} \omega_s b_s^\dagger b_s + \sum_{s=1}^{M} \kappa_{i,s}(b_s + b_s^\dagger)$$
$$+ \sum_{s,s'=1}^{M} \gamma_{i,ss'}(b_s + b_s^\dagger)(b_{s'} + b_{s'}^\dagger) \,, \tag{31}$$

where we have introduced a complex vertical resonance energy ϵ_i and complex vibrational coupling constants $\kappa_{i,s}, \gamma_{i,ss'}$,

$$\epsilon_i = \epsilon_i^R + i\epsilon_i^I \,,$$
$$\kappa_{i,s} = \kappa_{i,s}^R + i\kappa_{i,s}^I \,, \tag{32}$$
$$\gamma_{i,ss'} = \gamma_{i,ss'}^R + i\gamma_{i,ss'}^I \,.$$

In terms of the previously introduced quantities the real and imaginary parts of ϵ, κ, and γ are given by

$$\epsilon_i^R = \epsilon_i^0(0) + \Delta_i(0) \,, \quad \epsilon_i^I = -\tfrac{1}{2}\Gamma_i(0) \,, \tag{33a}$$

$$\kappa_{i,s}^R = \kappa_{i,s}^0 + \frac{1}{\sqrt{2}} \left(\frac{\partial \Delta_i}{\partial Q_s}\right)_0 ,$$

$$\kappa_{i,s}^I = -\frac{1}{2\sqrt{2}} \left(\frac{\partial \Gamma_i}{\partial Q_s}\right)_0 , \tag{33b}$$

$$\gamma_{i,ss'}^R = \gamma_{i,ss'}^0 + \frac{1}{4} \left(\frac{\partial^2 \Delta_i}{\partial Q_s \partial Q_{s'}}\right)_0 ,$$

$$\gamma_{i,ss'}^I = -\frac{1}{8} \left(\frac{\partial^2 \Gamma_i}{\partial Q_s \partial Q_{s'}}\right)_0 . \tag{33c}$$

The relevant equations which are used in the following are Eqs. (30) and (31). Starting from the Hamiltonian (8), which describes the coupling of a molecular quasiparticle level of positive energy to both the nuclear vibrations and the continuum of scattering states, and eliminating the electronic degrees of freedom within the adiabatic approximation, the non-Hermitian effective boson Hamiltonian (31) has been generated. The calculation of the vibrational cross sections has thus been reduced to a pure boson problem. The complex resonance energy and coupling constants

appearing in the effective Hamiltonian are by Eqs. (33), and Eqs. (28) and (29) uniquely related to the quantities characterizing the initial Hermitian Hamiltonian (8).

It remains to evaluate the squared matrix element in Eq. (30). This is most conveniently done by introducing a second quantization formalism for the multidimensional harmonic oscillator with complex potential energy, i.e., creation and annihilation operators for complex vibrational quanta. The details of the calculation and the general solution are given in the appendix. Here we quote only the final result for the most simple case of linear coupling ($\gamma = 0$) and one vibrational coordinate

$$\sigma(n, \epsilon_p) \sim \frac{|p'|}{|p|} \left| \sum_m \frac{A_{nm}}{\epsilon_p - \epsilon + \kappa^2/\omega - m\omega} \right|^2 ,$$

$$A_{nm} = e^{-a/2} (-1)^{n-m} \frac{1}{\sqrt{n!}} \left(\frac{\kappa}{\omega}\right)^n L_m^{n-m}(a) , \quad \text{for } m \leq n ,$$

$$= e^{-a/2} \frac{\sqrt{n!}}{m!} \left(\frac{\kappa}{\omega}\right)^{2m-n} L_n^{m-n}(a) , \quad \text{for } m \geq n , \qquad (34)$$

where $a = (\kappa/\omega)^2$ and L_n^m denotes the generalized Laguerre polynomial.[48] In the case of linear coupling to several normal vibrations the matrix elements of the T operator are given by Eqs. (A20) and (A24). In the general case of linear and quadratic coupling to several vibrational coordinates the result is given by Eqs. (A20) and (A21).

We have thus arrived at explicit algebraic expressions for the vibrational-excitation cross sections. In this respect the present approach differs from the theory of Birtwistle and Herzenberg,[14] which requires the numerical solution of the Schrödinger equation for a complex potential. This difference is of particular importance when more than one vibrational coordinate is considered, since the numerical solution of the nuclear wave equation is hardly possible in the multidimensional case. Physically, the present theory is closely related to the approach of Birtwistle and Herzenberg in that the compound-state picture[14] is adopted and the scattering problem reduced to the problem of vibrational motion in a complex adiabatic potential. The relationship between the compound-state approach, the adiabatic-nuclei theory,[17] and the hybrid theory of Chandra and Temkin[23] has been recently discussed by Schneider.[49]

III. APPLICATIONS

As mentioned in the Introduction, the vibrational phenomena associated with resonances depend on the relative magnitude of the resonance width Γ and the vibrational frequency ω. The theory developed in the preceding sections is, of course, applicable for arbitrary values of Γ and ω and comprises both limiting cases $\Gamma \ll \omega$ and $\Gamma \gg \omega$. A simplified treatment of these limiting cases has been given recently,[50] showing that the strength of vibrational excitation is determined by $(\kappa^0/\omega)^2$ in the limit $\Gamma \ll \omega$, whereas in the opposite limit $\Gamma \gg \omega_s$, it is given by $(\kappa^0/\Gamma)^2$ [see Eq. (7) for the definition of κ^0]. Here we concentrate on the intermediate case $\Gamma \approx \omega$, which has already received much attention in the literature.[12,14,15,51] Two examples which have been extensively investigated experimentally are the 2.4-eV resonance in N_2 and the 3.8-eV resonance in CO_2. Both resonances are of considerable practical interest in connection with the CO_2 laser.[52] The resonance in CO_2 will be first dealt with, treating the complex resonance energy ϵ and the complex coupling constant κ [defined in Eqs. (32) and (33)] as adjustable parameters. As a result of the smallness of the anharmonic constant of the symmetric-stretching coordinate of CO_2,[60] we expect the present harmonic theory to give good results. To be able to study the influence of anharmonicity we further consider the 2.4-eV resonance in N_2, where anharmonic effects are significant.[14] For N_2 the coupling constants required within the present approach can be determined from existing data, allowing the calculation of the vibrational-excitation functions without any adjustable parameter. Therefore, the influence of anharmonic effects can be quantitatively assessed by comparing the results of the harmonic theory with experiment. It will be shown how to extend the harmonic theory to partly include anharmonicity.

A. 3.8-eV resonance in CO_2

The 3.8-eV resonance in CO_2 has been observed in electron transmission[53,54] and elastic scattering[55] experiments. The vibrational excitation of CO_2 via the 3.8-eV resonance has been investigated by Boness and Schulz,[15,56] Danner,[57] and Cadez *et al.*[16] The theoretical work on this resonance is relatively scarce. Potential energy curves for the CO_2^- system have been computed by Claydon *et al.*[37] and by Krauss and Neumann.[36] Morrison *et al.*[21] computed total and momentum-transfer cross sections, neglecting, however, the vibrational motion. The angular distributions of the vibrationally inelastic scattered electrons have been calculated by Andrick and Read.[58]

The experimental situation is complicated by the fact that nonresonant vibrational excitation is also present in the case of CO_2. Both the antisymmetric stretching (ν_3) and the bending mode (ν_2) are excited via the dipole mechanism.[15,59] Direct excitation of the symmetric stretching

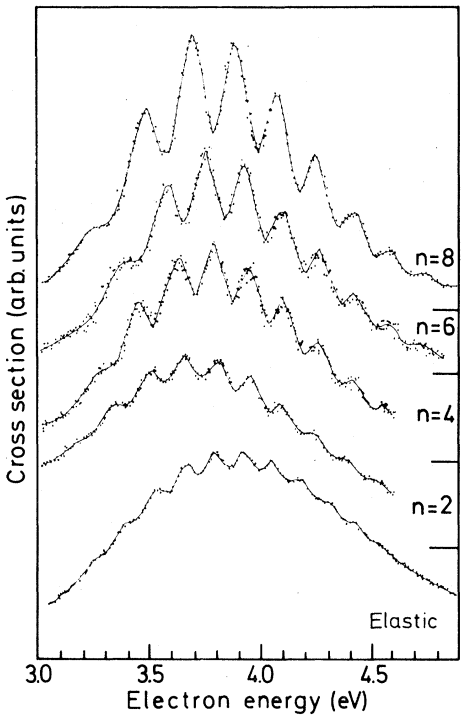

FIG. 1. Excitation functions for symmetric-stretch vibrational channels of the ground state of CO_2 measured at a scattering angle of 20° (after Čadež *et al.* in Ref. 16). The channel and the ordinate zero for each curve are indicated on the right. (Arbitrary ordinate scale for each channel.)

vibration (ν_1), which is dipole inactive, has been found to be extremely weak.[44,50]

In the resonance region, from 3 to 5 eV, excitation of the symmetric-stretching mode dominates. Resonant excitation of the bending mode is also observed.[15,16] This is not unexpected, since the calculations[36,37] predict a significant increase in the CO distance and a nonlinear equilibrium configuration for CO_2^- in its ground state. The linear-nonlinear transition occurring upon electron attachment to CO_2 cannot be treated within a harmonic theory. We therefore omit the bending coordinate and consider only the vibrational motion in the stretching coordinate. This is justified as long as the excitation functions for the symmetric-stretching vibrational channels are considered. Since the bending vibrational frequency is definitely smaller than the resonance width Γ[15,16] and since the force on the nuclei vanishes at the initial state equilibrium geometry, only small deviations from the linear conformation are expected to occur during the lifetime of the compound state. Indeed, we shall see that the measured excitation functions for the symmetric-stretch channels can be reproduced by considering only the symmetric stretching coordinate.

The excitation functions for the symmetric-stretch vibrational channels $n = 0, 2, 4, 6, 8$ as measured by Čadež *et al.*[16] are shown in Fig. 1. As noted by Čadež *et al.* the outstanding features are the regularity of the oscillations of the cross sections with the incident electron energy and the steady increase in the peak separation and the relative intensity of the oscillations with the channel number n. The whole phenomenon is similar to that observed in N_2 around 2.4 eV and extensively discussed in the literature (see below). It has been recognized[12] that the above mentioned behavior of the cross sections cannot be simply understood within the compound-state model, where the peaks are expected to occur at the vibrational levels of the compound state and thus should be independent of the exit channel.

When applying the theory developed in the preceding sections it is natural to first approach the problem within the linear-coupling approximation, i.e., to use the very simple formula (34) to calcu-

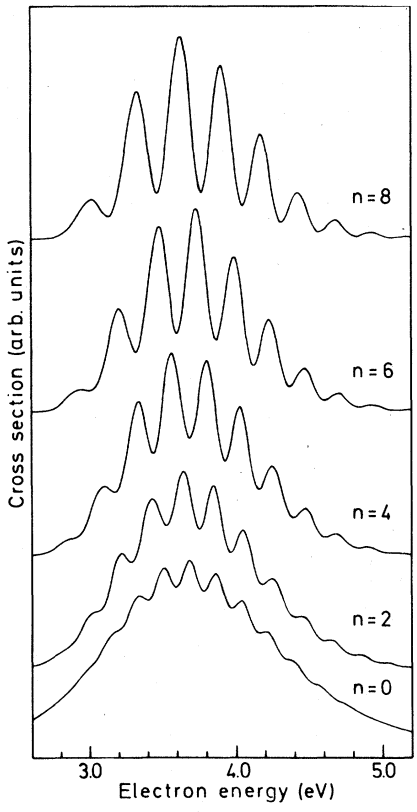

FIG. 2. Excitation functions for the symmetric-stretch vibrational channels $n = 0$, 2, 4, 6, 8 of the ground state of CO_2 calculated with Eq. (34) and $\epsilon^R = 3.80$ eV, $\epsilon^I = -0.27$ eV, $\kappa^R = -0.40$ eV, $\kappa^I = 0.03$ eV. (Arbitrary ordinate scale for each channel.)

late the vibrational excitation functions. This equation contains four adjustable parameters: the real and imaginary parts, ϵ^R and ϵ^I, of the vertical resonance energy ϵ, and the real and imaginary parts of the coupling constant, κ^R and κ^I. ϵ^R merely determines the position of the resonance on the energy scale. We are therefore left with three parameters which determine the structure and relative intensity of the vibrational excitation functions. The ground-state symmetric-stretching vibrational frequency ω is well known for CO_2 ($\omega = 1354\ \mathrm{cm}^{-1} = 0.168$ eV).[60]

Figure 2 shows the excitation functions for the symmetric-stretch vibrational channels $n = 0, 2, 4, 6, 8$ calculated with Eq. (34) and $\epsilon^R = 3.80$ eV, $\epsilon^I = -0.27$ eV, $\kappa^R = -0.40$ eV, $\kappa^I = 0.03$ eV. The values of the parameters $\epsilon^I, \kappa^R, \kappa^I$ were determined as follows. We first put κ^I equal to zero. ϵ^I then determines the width of the individual peaks, as can be seen from Eq. (34). From test calculations, it is found that κ^R determines the strength of vibrational excitation in the resonant-scattering process, i.e., the dependence of the cross section on the final-state vibrational quantum number n as well as the number of peaks in the excitation functions. With a suitable choice of ϵ^I we can thus fix κ^R by reproducing the observed number of peaks in the various excitation functions. Next, we vary κ^I. As shown in detail below, κ^I is responsible for the peculiar regular structure of the excitation functions. The structure of the excitation functions is rather sensitive to changes in κ^I. Therefore κ^I can be determined accurately from the fit to the experimental data. Since κ^I contributes to the width of the individual peaks [see Eq. (34)], ϵ^I has finally to be readjusted. The cross sections for the different channels have been individually normalized to equal maximum intensity, since no data on the relative magnitude of the cross sections for the various channels are reported by Čadež *et al.*[16] We therefore confine ourselves to the study of the energy dependence of $\sigma(n, \epsilon_p)$.

From Figs. 1 and 2, it is seen that all relevant features of the experimental curves are reproduced by the calculation. The calculated excitation functions show the observed highly regular oscillatory behavior, the decrease in the number of peaks with the corresponding increase in peak separation for increasing n, and the marked increase in the intensity of the oscillations for higher channel numbers. Obviously the linear-coupling approximation is sufficient to explain the experiment. The peaks in the calculated excitation functions are somewhat better resolved than in the experimental curves due to the larger peak spacing in the calculated functions. This larger spacing results from the neglect of anharmonic effects and of the change of vibrational frequency upon electron attachment in the linear-coupling approximation.

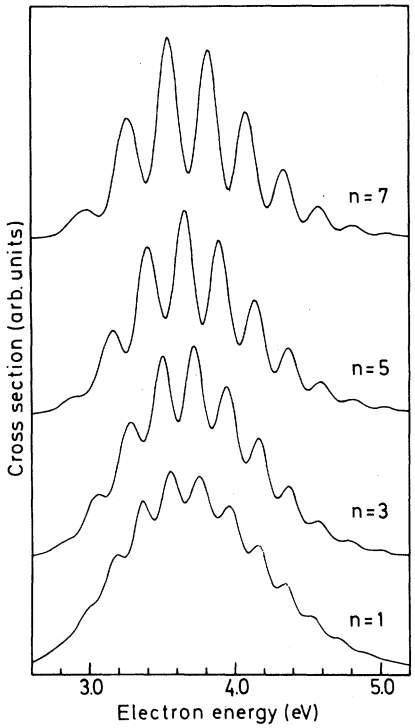

FIG. 3. Excitation functions for the symmetric-stretch vibrational channels $n = 1, 3, 5, 7$ of the ground state of CO_2 calculated with Eq. (34). The parameters are the same as in Fig. 2. (Arbitrary ordinate scale for each channel.)

The excitation functions calculated for the odd n channels up to $n = 7$ with Eq. (34) and the above choice of parameters are shown in Fig. 3. The general behavior of these functions is the same as that found for even n: the number of peaks decreases and the oscillatory structure becomes more pronounced with increasing channel number n. A closer examination reveals that the peaks in the odd n excitation functions are shifted systematically by about half a spacing against the peaks in the even n excitation functions.

It is interesting to compare these results with those obtained for $\kappa^I = 0$. Setting κ^I equal to zero means that the variation of the width Γ with the symmetric stretching coordinate is neglected. In this "constant Γ approximation," Eq. (34) reduces to the following expression used previously by various authors,[11,61,62]

$$\sigma(n, \epsilon_p) \sim \frac{|p'|}{|p|} \left| \sum_m \frac{\langle n | \hat{m} \rangle \langle \hat{m} | 0 \rangle}{\epsilon_p - \epsilon_0 - m\omega + \frac{1}{2} i\Gamma} \right|^2 , \qquad (35)$$

where $\langle n | \hat{m} \rangle$ and $\langle \hat{m} | 0 \rangle$ denote the usual overlap integrals between vibrational wave functions in the initial and the intermediate (resonant) electronic

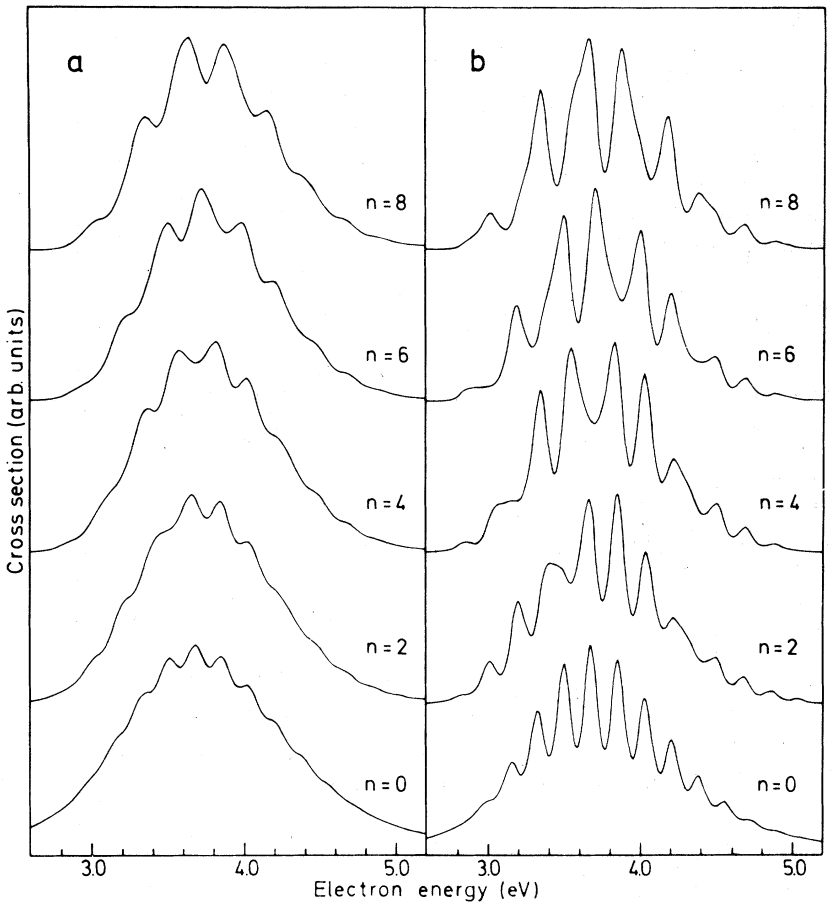

FIG. 4. (a) Excitation functions obtained with $\kappa^I = 0$ and $\epsilon^I = -0.125$ eV. ϵ^I has been chosen such that the excitation function for $n = 0$ is best reproduced. (b) Excitation functions obtained with $\kappa^I = 0$ and $\epsilon^I = -0.07$ eV. ϵ^I has been chosen such that the excitation function for $n = 8$ is best reproduced.

state and $\epsilon_0 = \epsilon^R - (\kappa^R)^2/\omega$ is the energy of the zeroth vibrational level in the resonance state.

In Fig. 4 the excitation functions for even n calculated within the constant Γ approximation are shown. The best fit to the elastic cross section within the constant Γ approximation is obtained with $\epsilon_I = -0.125$ eV ($\Gamma = 0.25$ eV) and $\kappa^R = -0.40$ eV as above. The corresponding excitation functions are shown in Fig. 4(a). The functions correctly show the decrease in peak number and the increase in peak separation with increasing n; they fail, however, to exhibit the marked increase in intensity of the oscillations with increasing n. Moreover, the oscillations of the excitation functions in Fig. 4(a) are not as regular as experimentally observed.

Figure 4(b) displays the excitation functions obtained with $\epsilon^I = -0.07$ eV ($\Gamma = 0.14$ eV). This value has been chosen such that the cross section for $n = 8$ is best reproduced. With this choice of ϵ^I, however, the peaks in the excitation functions for the lower n channels are considerably narrower than in the experiment. In addition, the inherent irregularity of the oscillations of the inelastic excitation functions becomes evident. It is thus clear that the observed structure of the excitation functions cannot be explained within the constant Γ approximation. No traces of irregularities are detectable in the excitation functions of Figs. 2 and 3 obtained with a small imaginary part of κ.

Let us now consider the positions of the peaks of the excitation functions for different channels in some more detail. It has become customary to plot the observed peak positions against the vibrational channel number.[15,16,51,63] The pattern observed by Čadež *et al.*[16] for CO_2 is shown in Fig. 5. The figure exhibits the regular increase in the separation of the peaks with increasing channel number. The calculated peak positions are shown in Fig. 6. Figure 6(a) displays the peak pattern obtained with $\kappa^I = 0.03$ eV, whereas Fig. 6(b) shows the pattern obtained in the constant Γ approximation, $\kappa^I = 0$. Corresponding peaks in different channels have been connected by lines to illustrate the movement of the peaks with the channel number n. For clarity, the peaks in the even n and odd n channels have been connected separately. As already mentioned, the peaks in the odd n channels

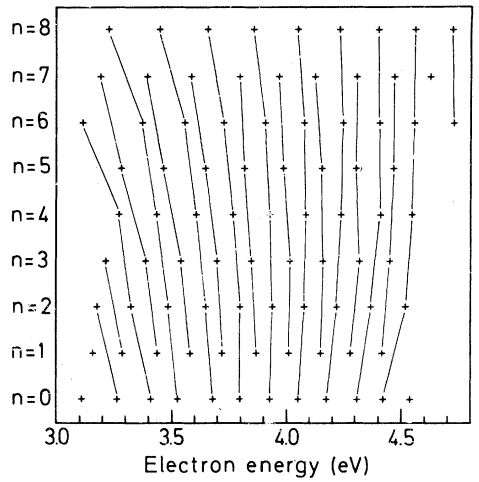

FIG. 5. Positions of the maxima observed in the excitation functions of the symmetric-stretch vibrational channels of CO_2 at 20° scattering angle (after Čadež *et al.* in Ref. 16).

are systematically displaced by half a spacing against the peaks in the even n channels.

It is seen that the qualitative behavior of the shifting of the peaks with the channel number is reproduced already in the constant Γ approximation [Fig. 6(b)]. The peaks are seen to move apart gradually, with a corresponding decrease in peak number. However, the spacing of the peaks in the inelastic channels is clearly irregular, in contrast to the rather regular pattern of Fig. 5. The peak pattern calculated with $\kappa^I = 0.03$ eV [Fig. 6(a)], on the other hand, exhibits a really perfect regularity and reproduces nicely the features observed experimentally.

The shifting of the maxima and minima of the cross sections with the channel number has received much attention in the literature.[12,14-16,51] The physically appealing "boomerang model" developed by Herzenberg[12] is generally adopted to explain the observed peak shifts. The model explains that the peaks appear in different channels at different energies and with different spacings. However, the model has sometimes been misinterpreted: the observed peak positions, plotted against the channel number as in Fig. 5, are usually connected by diagonal straight lines (see, e.g., Fig. 4 of Ref. 15, or Fig. 2 of Ref. 16). These lines seem to indicate a shifting of the peaks over several vibrational spacings as the channel number increases. This shifting is, however, not a true one. It is merely feigned by the systematic shift of the peaks in the odd n excitation functions against the peaks in the even n excitation functions discussed above. In particular, it is incorrect to assume that the diagonal lines usually drawn turn into vertical lines when the compound molecule limit $\Gamma \ll \omega$ is approached. The actual movement of the peaks is that shown in Figs. 5 and 6. Clearly the main effect is that the peaks *drift apart* with increasing channel number. Inspection of Fig. 4(b) reveals the origin of this behavior: with increasing n more and more of the vibrational peaks of the elastic channel are seen to vanish or to merge in neighboring ones. This is due to the increasing number of oscillations exhibited by the generalized Laguerre polynomials in Eq. (34) for real values of the coupling constant κ. The vanishing of peaks causes necessarily an irregular peak spacing. Inclusion of the imaginary part of κ smoothes out the irregularities in the cross sections and leads to the observed regular spacing of the peaks.

B. 2.4-eV resonance in N_2

The 2.4-eV resonance in N_2 is the molecular resonance which has been most extensively studied

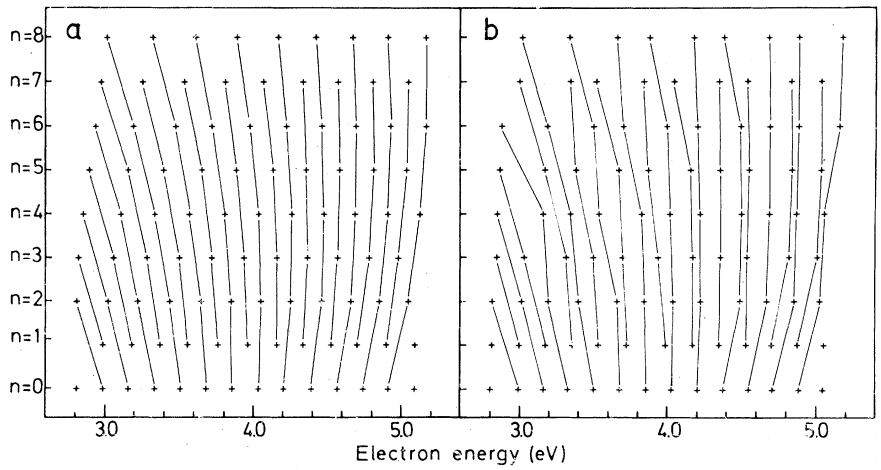

FIG. 6. Calculated positions of the maxima of the excitation functions of CO_2: (a) calculated with $\kappa^I = 0.03$ eV, (b) calculated with $\kappa^I = 0$.

both experimentally and theoretically. For a review of the work up to 1971, see Ref. 2. The peculiar oscillatory structure of the elastic and inelastic cross sections and the shift of the peak positions with the channel number first noted by Schulz[63] has stimulated considerable theoretical interest in the phenomenon. The early attempts[11,61,62] to explain the experimental observations, based on the constant Γ approximation, Eq. (35), could reproduce qualitatively some of the observed features, but were unable to explain the regularity of the oscillations and the shift of the positions of the cross section maxima and minima (see Ref. 14 for a detailed discussion of this earlier work). Accounting for the anharmonicity of the potential-energy curves by using Morse vibrational wave functions[61] did not lead to significant improvement over the results obtained in the harmonic approximation.[11,62]

The "boomerang model" of Herzenberg[12] was able to explain the observed peak shifts, but did not yield excitation functions to be compared with experiment. Birtwistle and Herzenberg[14] finally succeeded in developing a theory which was able to reproduce quantitatively the experimental facts. The essential new ingredient was to allow explicitly for a variation of the resonance width Γ with the internuclear distance R. Parametrizing the function $\Gamma(R)$ in a suitable way and approximating the real part $E^-(R)$ of the complex electronic energy of the N_2^- ion by a Morse function, Birtwistle and Herzenberg solved numerically for the vibrational wave function in the ionic state and calculated the overlap integrals with the vibrational wave function of the electronic ground state (approximated by appropriate Morse vibrational wave functions). By adjusting the parameters contained in $E^-(R)$ and $\Gamma(R)$ they obtained for all channels a quantitative fit to the observed excitation functions.

Ab initio calculations of $E^-(R)$ and $\Gamma(R)$ have also been performed,[23,64] yielding results in good agreement with the parametrization of Birtwistle and Herzenberg. In particular, the rapid decrease of Γ with increasing internuclear separation postulated by Birtwistle and Herzenberg has been confirmed by the *ab initio* calculations.

The recent hybrid theory of Chandra and Temkin[23] has allowed the calculation of absolute cross sections for both rotational and vibrational excitation. The vibrational substructure of the 2.4-eV resonance could be reproduced by a close-coupling calculation for the Π_g partial wave. The relationship between the close-coupling approach and the theories based on the compound-state picture[14] has been established by Schneider.[49]

After all this work the vibrational structure of the 2.4-eV shape resonance in N_2 is a well understood phenomenon. It represents, therefore, a useful example to study the possibilities and deficiencies of the present theory, especially with respect to the influence of anharmonicity. In contrast to the above discussed example of CO_2, where anharmonic effects play a minor role, anharmonicity is known to be important in the case of N_2.

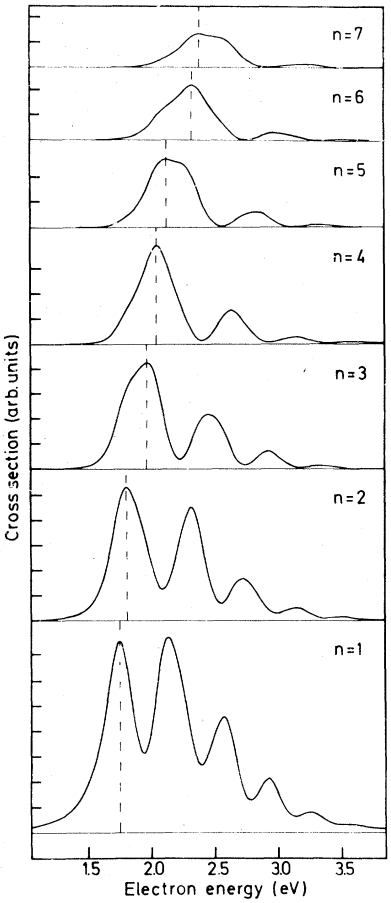

FIG. 7. Cross sections for resonant e-N_2 scattering calculated with Eq. (34). ϵ and κ have been determined from the parametrized resonance energy $E^-(R)$ and width $\Gamma(R)$ of Birtwistle and Herzenberg (Ref. 14). The ordinate scale is the same for all channels.

Knowing $E^-(R)$ and $\Gamma(R)$ from the parametrization of Birtwistle and Herzenberg,[14] we can calculate the required coupling constants. Restricting to the linear coupling approximation, we need only the two complex quantities ϵ and κ entering Eq. (34). With the data given in Ref. 14 we find

$$\epsilon^R = 2.35 \text{ eV}, \quad \epsilon^I = -0.285 \text{ eV},$$

$$\kappa^R = -0.382 \text{ eV}, \quad \kappa^I = 0.051 \text{ eV}.$$

The excitation functions obtained with these parameters are shown in Fig. 7. The ordinate scale is the same for all channels. Figure 7 thus exhibits the

dependence of the cross section on both the channel number n and the electron energy ϵ_p. The excitation functions of Fig. 7 should be compared with the experimental curves of Schulz[63] and Ehrhardt and Willmann[65] which are reproduced in Fig. 8.

The comparison with experiment shows that the dependence of the cross section on the channel number n is well described by the calculation. Moreover, the observed regularity of the oscillations of the excitation functions, which could not be understood within the constant Γ approaches,[11,61,62] is reproduced. Our results underline, in agreement with the results of Birtwistle and Herzenberg,[14] the necessity to account for the variation of Γ with the internuclear separation. As already found for CO_2 above, it is sufficient to consider the *linear* dependence of Γ on the internuclear distance [i.e., the leading term in the Taylor expansion of $\Gamma(R)$] in order to explain the regularity of the oscillations. Figure 7 exhibits also the observed shifting of the peaks to higher energy and the increase in peak spacing and peak width with increasing n. Similar to the resonance

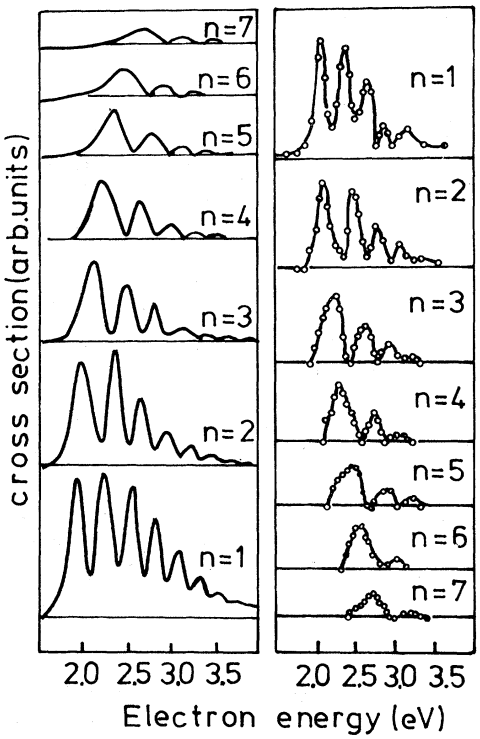

FIG. 8. Cross sections for resonant e-N_2 scattering measured by Ehrhardt and Willmann (Ref. 65) at a scattering angle of 20° and by Schulz (Ref. 63) at a scattering angle of 72°. Differences in the intensity distribution may be due to the different scattering angle or due to instrumental factors.

in CO_2 discussed above the relative intensity of the oscillations increases with the channel number.

Although the over-all agreement with experiment is remarkable in view of the simplicity of Eq. (34), there are several deficiencies which deserve a closer examination. Most obviously, the amplitude of the oscillations drops off too fast with increasing electron energy. It can be shown that this is an immediate consequence of the neglect of the anharmonicity of the negative-ion potential-energy curve $E^-(R)$ in our calculation. The same effect is observed when the vibrational structure for transitions between stationary electronic states is calculated within the harmonic approximation.[31-33] Apart from this too rapid drop-off of the oscillations, the calculated excitation functions up to $n = 4$ are in good agreement with experiment; even the detailed shape of the peaks is reproduced. For the higher n, however, the shape of the first broad peak is less well reproduced. In addition, the shift of the first peak with the channel number n is not in agreement with experiment. Upon closer examination the experimental peak positions show a systematic behavior (see Fig. 8): when going from an odd n to an even n channel, the first peak shifts only slightly to higher energy; going from an even n to an odd n channel, a large shift of the first peak is observed. As indicated by the dashed vertical lines, the cross sections in Fig. 7 exhibit this feature correctly up to $n = 4$, but not for the higher n. The fact that the excitation functions are for larger n less well reproduced by the present calculation is not surprising when keeping in mind that the final vibrational states $|n\rangle$ cannot be well described within the harmonic approximation for large n. The deficiencies in the excitation functions appearing for higher n are due to the neglect of the anharmonicity of the electronic ground state potential energy curve $E_0(R)$, whereas the general too rapid drop-off of the oscillations is due to the neglect of the anharmonicity of the potential energy curve $E^-(R)$ of N_2^-.

Before entering a more detailed discussion of anharmonic effects, it should be pointed out that the harmonic expansion on which the present theory is based is principally different from the harmonic expansion in its traditional form, as widely used for calculating Franck-Condon factors for electronic transitions.[13] In the traditional approach the potential energies of the two electronic states involved in the transition are expanded into a Taylor series about their *respective* minima. In the present approach, on the other hand, both potential energies are expanded about the *same* internuclear distance, namely the electronic ground-state equilibrium distance. In formulating a harmonic theory we are of course free to choose the point of ex-

pansion R_0 at our convenience. If the potential-energy curves were truly parabolic, the results would be the same for all choices of R_0. Since actual molecular potential functions are never parabolic, the results obtained within a harmonic theory depend on the choice of R_0. We can use this freedom in the choice of R_0 to obtain the "best" harmonic approximation for each problem in question (see Ref. 33 for a detailed discussion of this point in connection with the vibrational structure in photoelectron spectra).

In the resonant scattering process two electronic transitions are involved: the capture and the re-emission of the electron. With the first transition there is associated a vibrational overlap element $\langle 0|\bar{m}\rangle$ and with the second an overlap element $\langle \bar{m}|n\rangle$, where $|n\rangle$ denotes the vibrational states of the molecule in its electronic ground state and $|\bar{m}\rangle$ the vibrational states of the negative ion. These overlap elements determine, according to the Franck-Condon principle, the population of the vibrational states of the temporary negative ion and of the molecule after the scattering process. It can be shown that the optimum harmonic expansion for the calculation of the first overlap element $\langle 0|\bar{m}\rangle$ is to expand both the ground-state potential energy $E_0(R)$ and the complex negative-ion energy $E^-(R) - \frac{1}{2}i\Gamma(R)$ about the ground-state equilibrium geometry.

The vibrational wave function corresponding to the initial state $|0\rangle$ is fairly localized and defines a narrow Franck-Condon zone. It is the behavior of $E^-(R) - \frac{1}{2}i\Gamma(R)$ within this zone which determines the distribution of the transition probability over the vibrational states $|\bar{m}\rangle$. Therefore, the optimum choice for the expansion point is the center of the Franck-Condon zone. This choice is, however, not necessarily suitable for the calculation of the second overlap element $\langle \bar{m}|n\rangle$. If the final-state vibrational quantum number n is large, the corresponding vibrational wave function oscillates rapidly except in the vicinity of the classical turning points. In this case the relevant Franck-Condon zone is near one of the classical turning points and, by the same argument as above, the optimum choice for the expansion point R_0 is within this Franck-Condon zone. It is clear that with this choice of R_0 the first transition is less well described.

A useful compromise will be to choose the expansion point just midway between the above two extremes. Using in this way a different harmonic expansion for each channel n, we are in a position to account partly for the anharmonicity of the ground-state potential curve without losing the simplicity of the harmonic theory. The formulas derived in the appendix remain valid, but the parameters in these expressions now depend on the channel number n. Note that we have a fixed prescription to calculate this dependence of the parameters on the channel number, provided the potential energies of the molecule in its ground state and of the negative ion are given.

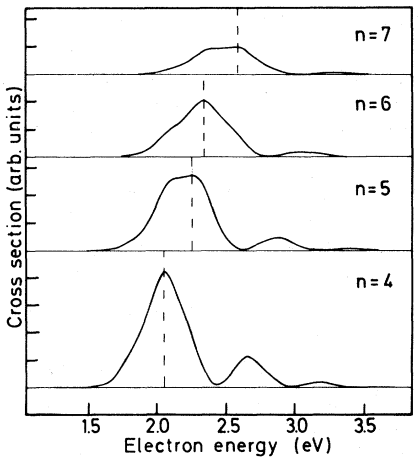

FIG. 9. Cross sections for resonant e-N_2 scattering obtained by using a different harmonic expansion for each channel n (see text). In contrast to Fig. 7, the shift of the first maximum with the channel number (indicated by the dashed vertical lines) is in agreement with the experimental observations.

We have performed such a calculation for N_2 using the parametrized potential functions of Birtwistle and Herzenberg.[14] The results are displayed in Fig. 9. The excitation functions for the lower inelastic channels $n = 1$ to 4 change only very slightly compared to Fig. 7 and are not drawn again. The higher excitation functions, however, exhibit distinct changes. For $n = 5$ and $n = 7$, in particular, the shape of the first broad peak is altered: the peak maximum moves from the left to the right hand side of the peak. The shape of the peaks is now in better agreement with experiment (see Fig. 8). Moreover, the shift of the first maximum with the channel number n is now in agreement with experiment. As indicated by the dashed vertical lines, there is a large shift from $n = 4$ to $n = 5$, a small shift from $n = 5$ to $n = 6$, and again a large shift from $n = 6$ to $n = 7$. This behavior was not exhibited by the excitation functions in Fig. 7.

We mention in passing that the anharmonicity of the real part $E^-(R)$ of the negative-ion potential function, which is responsible for the enhancement of the oscillations in the high-energy tail of the cross sections, can also be partly accounted for in a simple way: we just have to replace $m\omega$ in the denominator of Eq. (34) by $\sum_{\mu=1}^{m} \omega_\mu$ and ω in the numerator by ω_m, where ω_μ is the true spac-

ing between the $(\mu-1)$th and the μth vibrational level. The decrease of ω_m with increasing m causes a steady increase in κ/ω_m and leads to the required enhancement of the high-energy tail of the excitation functions.

We have also studied the influence of the quadratic coupling constant $\gamma=\gamma^R+i\gamma^I$ on the cross sections, using the general expression (A21). γ^R and γ^I are easily determined from $E^-(R)$ and $\Gamma(R)$ as given by Birtwistle and Herzenberg.[14] Both the real and the imaginary part of γ are an order of magnitude smaller than the corresponding part of the linear coupling constant κ. Neither the inclusion of γ^R nor that of γ^I was found to result in a significant improvement of the calculated excitation functions. This is due to the fact that for N_2 the influence of the quadratic coupling constant is of the same order of magnitude as the influence of the anharmonicity of the potential functions. It is in this case of little use to keep γ when neglecting the influence of the anharmonicity. Consideration of the quadratic coupling constant γ is essential, when the linear coupling constant vanishes due to symmetry requirements, as is the case, e.g., for the bending mode of CO_2.

IV. CONCLUSIONS

A simple Hamiltonian describing the coupling of a molecular quasiparticle state of positive energy to the continuum of scattering states as well as to the vibrational degrees of freedom has been formulated. Within the adiabatic approximation the perturbation series for the S matrix has been summed to infinite order in the bound-state–continuum interaction. Neglecting nonadiabatic effects and the energy dependence of the resonance width and shift, the vibrational motion in the resonant electronic state is described by an effective non-Hermitian boson Hamiltonian. Introducing a second quantization formalism adapted to describe the creation and annihilation of quanta of complex energy, the effective Hamiltonian could be diagonalized and the vibrational cross sections calculated exactly. Particularly simple expressions are obtained when only linear coupling to the vibrational motion is considered.

The theory has been applied to the 3.8-eV shape resonance in CO_2 and the 2.4-eV shape resonance in N_2. In both cases, the resonance width is of the same order of magnitude as the vibrational frequency, resulting in an interesting and nontrivial energy and channel-number dependence of the cross section. The consideration of linear coupling is found to be sufficient for the understanding of the experimentally observed phenomena. For CO_2 it is found that the introduction of only one additional parameter, namely the imaginary part κ^I of the linear coupling constant, leads to a dramatic improvement over existing theories, which express the cross sections in terms of conventional Franck-Condon factors. The discussion of the N_2 molecule has been mainly devoted to a study of the influence of the anharmonicity of the potential functions. In contrast to CO_2, where the anharmonic constant for the symmetric stretching coordinate is small,[60] anharmonic effects are significant for N_2. It has been shown how the anharmonic nature of the potential curves can be qualitatively accounted for even within a harmonic theory by choosing the optimum point of expansion.

Our results are in full accord with those of Birtwistle and Herzenberg[14] who first pointed out that it is the rapid variation of the resonance width Γ with the internuclear distance which is responsible for the regularity of the oscillations in the inelastic cross sections of N_2 near 2.4 eV. In contrast to the work of Birtwistle and Herzenberg, which is purely numerical, the present theory supplies us with simple and explicit expressions which can be used with negligible computational effort to reproduce or to predict vibrational-excitation cross sections. In particular, the theory is easily applicable to polyatomic molecules with more than one totally symmetric normal vibration. Most of the experimental work at present is concerned with such molecules.[3-8]

An extension of the theory is necessary in order to deal with couplings to nontotally symmetric vibrations accompanied by a lowering of the symmetry of the molecule (CO_2, for example, becomes nonlinear[36,37] and H_2CO nonplanar[66] upon electron attachment). These processes cannot be described within the harmonic approximation. Another interesting phenomenon, which can be included by an appropriate extension[33] of the Hamiltonian (8), is the coupling of a degenerate level to Jahn-Teller active modes. An example is provided by the first shape resonance in benzene.[4]

A final comment concerns the *ab initio* determination of the complex coupling constants. Methods to calculate potential energy curves and widths for resonance states have been described in the literature and applied to diatomic and small polyatomic molecules.[23,36-40,64,66] These methods can be used to calculate the complex resonance energy ϵ and the complex coupling constants, but may turn out to be too expensive to be applied to larger polyatomic molecules. We suggest that for shape resonances a crude estimate of the quantity κ^R, which governs the strength of the vibrational excitation and the number of peaks in the excitation functions, may be obtained by neglecting the term $2^{-1/2}(\partial\Delta/\partial Q)_0$ in Eq. (33b) and by approximating

κ^0 by the derivative of the corresponding Hartree-Fock virtual orbital energy $2^{-1/2}(\partial\epsilon_i/\partial Q)_0$. For CO_2, for example, we obtain from the near Hartree-Fock-limit data of McLean and Yoshimine[67] $\kappa^R = -0.39$ eV, in excellent agreement with the value -0.40 eV obtained from the fit to the experimental cross sections. For N_2, the result of a Hartree-Fock calculation[68] using a Gaussian basis set without polarization functions is $\kappa^R = -0.44$ eV compared to the value -0.38 eV resulting from the parametrization of Birtwistle and Herzenberg[14] and the value -0.46 eV following from the calculation of Krauss and Mies[64] on N_2^-. The fact that the vibrational coupling for the first shape resonance of CO_2 is much stronger than for the corresponding resonance of N_2 is thus clearly explained. Although it is known that the Hartree-Fock virtual orbital energies are poor approximations to the resonance energies, it seems that the strength of the coupling of the resonance to the nuclear vibrations can be qualitatively inferred from the corresponding Hartree-Fock virtual orbital, at least for the lowest shape resonance. Of course a careful choice of the basis set is necessary to obtain reliable results. Our conjecture is supported by the recent study of Ökzan *et al.*[66] on formaldehyde, who found an almost exact parallelism between the $2b_1$ orbital energies calculated for H_2CO and H_2CO^-, respectively.

APPENDIX: THE COMPLEX HARMONIC OSCILLATOR

To simplify the calculation the following matrix notation is used. Let κ denote the M-dimensional vector of linear coupling constants $\kappa_{i,s}$ and $\underline{\gamma}$ the matrix of quadratic coupling constants $\gamma_{i,ss'}$. We then define the $2M$-dimensional vectors and matrices

$$\underline{K} = \begin{pmatrix} \underline{\kappa} \\ \underline{\kappa} \end{pmatrix}, \quad \underline{\Gamma} = \begin{pmatrix} \underline{\gamma} & \underline{\gamma} \\ \underline{\gamma} & \underline{\gamma} \end{pmatrix}, \quad \underline{\Omega} = \begin{pmatrix} \underline{\omega} & 0 \\ 0 & \underline{\omega} \end{pmatrix}, \tag{A1}$$

$$\underline{B} = \begin{pmatrix} b_1 \\ \vdots \\ b_M \\ b_1^\dagger \\ \vdots \\ b_M^\dagger \end{pmatrix},$$

where $\underline{\omega}$ is the diagonal matrix of vibrational frequencies introduced above. With these definitions, the Hamiltonian (31) takes the form

$$\mathcal{H} = \tfrac{1}{2}\underline{B}^\dagger\underline{\Omega}\underline{B} + \underline{B}^\dagger\underline{K} + \underline{B}^\dagger\underline{\Gamma}\underline{B} + \epsilon_i - \tfrac{1}{4}\,\mathrm{tr}\underline{\Omega}\,. \tag{A2}$$

We now consider new boson creation and annihilation operators related to new (complex) coordinates $\overline{Q}_s$ by

$$\begin{aligned} c_{\overline{\omega}_s} &= \frac{1}{\sqrt{2}}\left(\overline{Q}_s + \frac{\partial}{\partial \overline{Q}_s}\right), \quad c^\dagger_{\overline{\omega}_s} = \frac{1}{\sqrt{2}}\left(\overline{Q}^*_s - \frac{\partial}{\partial \overline{Q}^*_s}\right), \\ c_{\overline{\omega}^*_s} &= \frac{1}{\sqrt{2}}\left(\overline{Q}^*_s + \frac{\partial}{\partial \overline{Q}^*_s}\right), \quad c^\dagger_{\overline{\omega}^*_s} = \frac{1}{\sqrt{2}}\left(\overline{Q}_s - \frac{\partial}{\partial \overline{Q}_s}\right). \end{aligned} \tag{A3}$$

The index $\overline{\omega}_s, \overline{\omega}^*_s$ on the operators $c^\dagger, c$ denotes the type of quanta created or annihilated by these operators. Because these quanta are complex, four types of operators are necessary instead of two (b_s and $b_s^\dagger$) in the real case. Furthermore, one has to distinguish between right-hand side (rhs) and left-hand side (lhs) states. These rhs and lhs states are defined by

$$\begin{aligned} c_{\overline{\omega}_s}|\ldots \overline{n}_s \ldots\rangle &= (n_s)^{1/2}|\ldots \overline{n}_s - \overline{1} \ldots\rangle, \\ c^\dagger_{\overline{\omega}^*_s}|\ldots \overline{n}_s \ldots\rangle &= (n_s+1)^{1/2}|\ldots \overline{n}_s + \overline{1} \ldots\rangle, \\ \langle \ldots \overline{n}_s \ldots | c^\dagger_{\overline{\omega}^*_s} &= (n_s)^{1/2}\langle \ldots \overline{n}_s - \overline{1} \ldots |, \\ \langle \ldots \overline{n}_s \ldots | c_{\overline{\omega}_s} &= (n_s+1)^{1/2}\langle \ldots \overline{n}_s + \overline{1} \ldots |. \end{aligned} \tag{A4}$$

It will now be shown that the operators $c, c^\dagger$ can be chosen to diagonalize $\mathcal{H}$, the states (A4) being the rhs and lhs eigenstates of the non-Hermitian operator $\mathcal{H}$. In analogy to Eq. (A1), we define the $2M$-dimensional vector

$$\underline{C} = \begin{pmatrix} c_{\overline{\omega}_1} \\ \vdots \\ c_{\overline{\omega}_M} \\ c^\dagger_{\overline{\omega}^*_1} \\ \vdots \\ c^\dagger_{\overline{\omega}^*_M} \end{pmatrix} \tag{A5a}$$

and its transpose

$$\underline{C}^T = (C^\dagger)^* = (c^\dagger_{\overline{\omega}^*_1} \ldots c^\dagger_{\overline{\omega}^*_M} c_{\overline{\omega}_1} \ldots c_{\overline{\omega}_M}). \tag{A5b}$$

The new operators $c, c^\dagger$ are supposed to be related to the $b, b^\dagger$ according to

$$\underline{C} = \underline{\Lambda}\,\underline{B} \tag{A6}$$

with a complex matrix

$$\underline{\Lambda} = \begin{pmatrix} \underline{\lambda}_1 & \underline{\lambda}_2 \\ \underline{\lambda}_2 & \underline{\lambda}_1 \end{pmatrix}. \tag{A7}$$

Requiring the $c, c^\dagger$ to obey the commutation relations for bosons leads to

$$\underline{\Lambda}^{-1} = \begin{pmatrix} \underline{\lambda}_1^T & -\underline{\lambda}_2^T \\ -\underline{\lambda}_2^T & \underline{\lambda}_1^T \end{pmatrix}. \tag{A8}$$

We now choose $\underline{\Lambda}$ to diagonalize $\mathcal{H}$, i.e., to give

$$\mathcal{H} = \tfrac{1}{2}\underline{C}^T\underline{\bar{\Omega}}\,\underline{C} + \underline{C}^T\underline{\bar{K}} + \epsilon_i - \tfrac{1}{4}\,\mathrm{tr}\underline{\Omega}\,, \tag{A9}$$

with $\underline{\bar{\Omega}}$ and $\underline{\bar{K}}$ defined in analogy to $\underline{\Omega}$ and $\underline{K}$. From Eqs. (A2) and (A6)–(A9) we find

$$\underline{J}^T\underline{\bar{\omega}}\,\underline{J} = \underline{\omega} + 4\underline{\gamma}\,, \tag{A10}$$

$$\underline{\bar{\omega}} = \underline{J}\,\underline{\omega}\,\underline{J}^T\,, \tag{A11}$$

$$\underline{\bar{K}} = \underline{J}^{-1T}\underline{K} \tag{A12}$$

with

$$\underline{J} = \underline{\lambda}_1 + \underline{\lambda}_2\,. \tag{A13}$$

The general solution of Eq. (A11) is

$$\underline{J} = \underline{\bar{\omega}}^{1/2}\underline{Z}\,\underline{\omega}^{-1/2} \tag{A14}$$

with

$$\underline{Z}\,\underline{Z}^T = \underline{1}\,. \tag{A15}$$

Inserting Eq. (A14) into Eq. (A10) we obtain

$$\underline{\omega}^{1/2}(\underline{\omega} + 4\underline{\gamma})\underline{\omega}^{1/2}\underline{Z}^T = \underline{Z}^T\underline{\bar{\omega}}^2\,. \tag{A16}$$

Eq. (A16) is the eigenvalue problem for a complex symmetric matrix. It can be shown that the complex eigenvectors are orthogonal and can be normalized, provided that the eigenvalues are nonzero and not accidentally degenerate. Thus, $\underline{Z}\,\underline{Z}^T = 1$, as required for Eq. (A14) to be a solution of Eq. (A11). The eigenvalues $\bar{\omega}_s$ represent complex vibrational frequencies. We have thus shown that the Hamiltonian $\mathcal{H}$, which governs the nuclear motion in the intermediate state, describes a shifted [due to the linear term in Eq. (A9)] harmonic oscillator with complex frequencies. The eigenvector matrix $\underline{Z}$ determines via Eqs. (A14), (A13), and (A6) the creation and annihilation operators $c^\dagger$, c and thus the rhs and lhs eigenstates (A4) of H.

The M-dimensional complex symmetric eigenvalue problem (A16) can be replaced by the eigenvalue problem of a real nonsymmetric matrix of dimension $2M$. Writing the complex symmetric matrix $\underline{A}$ as $\underline{A} = \underline{B} + i\underline{C}$, the problem

$$\underline{A}\,\underline{X} = \underline{X}\,\underline{\Lambda}$$

can be replaced by

$$\begin{pmatrix} \underline{B} & -\underline{C} \\ \underline{C} & \underline{B} \end{pmatrix}\begin{pmatrix} \underline{X} & \underline{X}^* \\ -i\underline{X} & i\underline{X}^* \end{pmatrix} = \begin{pmatrix} \underline{X} & \underline{X}^* \\ -i\underline{X} & i\underline{X}^* \end{pmatrix}\begin{pmatrix} \underline{\Lambda} & 0 \\ 0 & \underline{\Lambda}^* \end{pmatrix}, \tag{A17}$$

which is closely related to the non-Hermitian eigenvalue problems occurring in RPA theories.[69]

It should be pointed out that the calculation leading to Eq. (A16) is a straightforward generalization of the calculation of Franck-Condon factors for electronic transitions between stationary electronic states as outlined in Ref. 32. The sole difference is that complex quantities appear instead of the usually real coupling constants, frequencies, etc. It is the advantage of the second quantization formalism that the calculation of overlap matrix elements between vibrational wave functions reduces to purely algebraic manipulations, which of course can be done with complex quantities as well.

It remains to eliminate the shift term $\underline{C}^T\underline{\bar{K}}$ in the Hamiltonian (A9). This is performed by the nonunitary transformation

$$U = \exp\left(-\sum_s \frac{\bar{K}_s}{\bar{\omega}_s}(c_{\bar{\omega}_s} - c^\dagger_{\bar{\omega}_s}{}^*)\right), \tag{A18}$$

giving

$$U\mathcal{H}U^{-1} = \sum_{s=1}^{M} \bar{\omega}_s c^\dagger_{\bar{\omega}_s}{}^* c_{\bar{\omega}_s} + \epsilon_i - \sum_{s=1}^{M} \frac{\bar{K}_s^2}{\bar{\omega}_s} + \frac{1}{2}\sum_{s=1}^{M}(\bar{\omega}_s - \omega_s)\,. \tag{A19}$$

Inserting the complete set of eigenstates of $\mathcal{H}$, the matrix element of T in Eq. (30) becomes

$$\langle n_1 \ldots n_M | V_{p'i}(\epsilon_p - \mathcal{H})^{-1} V_{ip} | \vec{0} \rangle = \sum_{m_1 \ldots m_M} \langle n_1 \ldots n_M | V_{p'i} U^{-1} | \bar{m}_1 \ldots \bar{m}_M \rangle \langle \bar{m}_1 \ldots \bar{m}_M | U V_{ip} | \vec{0} \rangle \times \left(\epsilon_p - \epsilon_i + \sum_s \frac{\bar{K}_s^2}{\bar{\omega}_s} - \frac{1}{2}\sum_s (\bar{\omega}_s - \omega_s) - \sum_s m_s \bar{\omega}_s\right)^{-1}. \tag{A20}$$

We neglect in the following the dependence of V_{ip} and $V_{p'i}$ on the nuclear coordinates $\vec{Q}$. This corresponds to the well-known Condon approximation in the theory of electronic transitions. Corrections to this approximation can easily be obtained by expanding V_{ip} and $V_{p'i}$ in powers of $\vec{Q}$.

We are thus left with the evaluation of the matrix elements of U and U^{-1}. This evaluation follows completely the lines given in Ref. 32 and need not be repeated here. The final result is

$$\langle n_1 \ldots n_M \,|\, U^{-1} \,|\, \bar{m}_1 \ldots \bar{m}_M \rangle$$

$$= \exp(\tfrac{1}{2}\underline{\beta}^T \underline{\lambda}_1 \underline{\alpha}) \sum_{\mu_1=0}^{m_1} \cdots \sum_{\mu_M=0}^{m_M} \sum_{\nu_1=0}^{n_1} \cdots \sum_{\nu_M=0}^{n_M} \left\{ \prod_{j=1}^{M} \left[\frac{1}{\nu_j!} \binom{n_j}{\nu_i} \right]^{1/2} \alpha_j^{\nu_j} \right\} \left\{ \prod_{j=1}^{M} \left[\frac{1}{\mu_j!} \binom{m_j}{\mu_j} \right]^{1/2} \beta_j^{\mu_j} \right\} \langle \ldots n_s - \nu_s \ldots | \ldots \bar{m}_s - \bar{\mu}_s \ldots \rangle \tag{A21}$$

and

$$\langle \bar{m}_1 \ldots \bar{m}_M \,|\, U \,|\, n_1 \ldots n_M \rangle = \langle n_1 \ldots n_M \,|\, U^{-1} \,|\, \bar{m}_1 \ldots \bar{m}_m \rangle \, .$$

The α_j and β_j are the elements of the complex vectors

$$\underline{\alpha} = -\underline{\lambda}_1^{-1} \underline{\bar{\omega}}^{-1} \underline{\bar{\kappa}} \, ,$$
$$\underline{\beta} = (1 - \underline{\lambda}_2 \underline{\lambda}_1^{-1}) \underline{\bar{\omega}}^{-1} \underline{\bar{\kappa}} \, . \tag{A23}$$

In Eq. (A21) the matrix elements of the shift operator U^{-1} have been expressed as a finite linear combination of the overlaps of the vibrational wave functions of the ground state and the *unshifted* wave functions of the intermediate state. These latter overlaps can be obtained from simple recursion relations which have been given in the appendix of Ref. 32.

Within the harmonic and Condon approximations Eqs. (A20) and (A21) give the complete solution of the vibrational problem. The expressions account not only for a shift of the equilibrium position of the intermediate state (represented by $\kappa_{i,s}^R$) and for changes in the vibrational frequencies and a distortion of the system of normal coordinates (represented by $\gamma_{i,ss'}^R$), but also for the variation of the resonance width Γ_i with Q_s and the coupling of normal coordinates through nondiagonal derivatives $(\partial^2 \Gamma_i / \partial Q_s \, \partial Q_{s'})$.

A considerable simplification occurs when the quadratic coupling constants $\gamma_{i,ss'}$ can be neglected and only the linear coupling is retained. In this case we have $\bar{\omega}_s = \omega_s$ (and thus real vibrational frequencies in the intermediate state) and Eq. (A21) reduces to

$$\langle n_1 \ldots n_M \,|\, U^{-1} \,|\, \bar{m}_1 \ldots \bar{m}_M \rangle$$

$$= \prod_{s=1}^{M} \left\{ e^{-a_s/2} \left(\frac{m_s!}{n_s!} \right)^{1/2} \left(-\frac{\kappa_s}{\omega_s} \right)^{n_s - m_s} L_{m_s}^{n_s - m_s}(a_s) \right\} \tag{A24a}$$

for $m_s \leq n_s$, and

$$\langle n_1 \ldots n_M \,|\, U^{-1} \,|\, \bar{m}_1 \ldots \bar{m}_M \rangle$$

$$= \prod_{s=1}^{M} \left\{ e^{-a_s/2} \left(\frac{n_s!}{m_s!} \right)^{1/2} \left(\frac{\kappa_s}{\omega_s} \right)^{m_s - n_s} L_{n_s}^{m_s - n_s}(a_s) \right\} \tag{A24b}$$

for $m_s \geq n_s$, where $a_s = (\kappa_s / \omega_s)^2$ and L_n^m denotes the generalized Laguerre polynomial.[48]

[1] G. J. Schulz, Rev. Mod. Phys. 45, 378 (1973).
[2] G. J. Schulz, Rev. Mod. Phys. 45, 423 (1973).
[3] I. Nenner and G. J. Schulz, J. Chem. Phys. 62, 1747 (1975).
[4] S. F. Wong and G. J. Schulz, Phys. Rev. Lett. 35, 1429 (1975).
[5] P. D. Burrow and K. D. Jordan, Chem. Phys. Lett. 36, 594 (1975).
[6] P. D. Burrow and J. A. Michejda, Chem. Phys. Lett. 42, 223 (1976); K. D. Jordan, J. A. Michejda, and P. D. Burrow, Chem. Phys. Lett. 42, 227 (1976).
[7] E. H. van Veen, W. L. van Dijk, and H. H. Brongersma, Chem. Phys. 16, 337 (1976).
[8] D. Mathur and J. B. Hasted, Chem. Phys. 16, 347 (1976).
[9] J. N. Bardsley and F. Mandl, Rep. Prog. Phys. 31, 471 (1968).
[10] H. S. Taylor, Adv. Chem. Phys. 18, 91 (1970).
[11] A. Herzenberg and F. Mandl, Proc. R. Soc. Lond. A270, 48 (1962).
[12] A. Herzenberg, J. Phys. B 1, 548 (1968).
[13] G. Herzberg, *Electronic Spectra and Electronic Structure of Polyatomic Molecules* (Van Nostrand, New York, 1966).
[14] D. T. Birtwistle and A. Herzenberg, J. Phys. B 4, 53 (1971).
[15] M. J. W. Boness and G. J. Schulz, Phys. Rev. A 9, 1969 (1974).
[16] I. Čadež, M. Tronc, and R. I. Hall, J. Phys. B 7, L132 (1974).
[17] A. Temkin and K. V. Vasavada, Phys. Rev. 160, 109 (1967).
[18] R. J. W. Henry and N. F. Lane, Phys. Rev. 183, 221 (1969).
[19] P. G. Burke and A. L. Sinfailam, J. Phys. B 3, 641 (1970); P. G. Burke and N. Chandra, J. Phys. B 5, 1696 (1972).
[20] B. I. Schneider, Phys. Rev. A 11, 1957 (1975); B. I. Schneider and P. J. Hay, J. Phys. B 9, L165 (1976).
[21] M. A. Morrison, L. A. Collins, and N. F. Lane, Chem. Phys. Lett. 42, 365 (1976).
[22] T. N. Rescigno, C. W. McCurdy, and V. McKoy, Phys. Rev. A 11, 825 (1975); C. W. McCurdy, T. N. Rescigno,

and V. McKoy, J. Phys. B 9, 691 (1976).
[23]N. Chandra and A. Temkin, Phys. Rev. A 13, 188 (1976); A 14, 507 (1976); J. Chem. Phys. 65, 4537 (1976).
[24]R. J. W. Henry, Phys. Rev. A 2, 1349 (1970).
[25]M. A. Brandt, D. G. Truhlar, and F. A. Van-Catledge, J. Chem. Phys. 64, 4957 (1976).
[26]H. Feshbach, Ann. Phys. (N.Y.) 5, 357 (1958); 19, 287 (1962).
[27]U. Fano, Phys. Rev. 124, 1866 (1961).
[28]Y. Hahn, T. F. O'Malley, and L. Spruch, Phys. Rev. 128, 932 (1962); T. F. O'Malley and S. Geltman, Phys. Rev. 137, A1344 (1965).
[29]A. S. Davydov, *Quantum Mechanics*, 2nd ed. (Pergamon, Oxford, 1976), Chaps. X and XI.
[30]D. J. Thouless, *The Quantum Mechanics of Many-Body Systems* (Academic, New York, 1961); A. Abrikosov, L. Gorkov, and J. Dzyaloshinskii, *Quantum Field Theoretical Methods in Statistical Physics* (Pergamon, Oxford, 1965).
[31]L. S. Cederbaum and W. Domcke, J. Chem. Phys. 60, 2878 (1974).
[32]L. S. Cederbaum and W. Domcke, J. Chem. Phys. 64, 603, 612 (1976).
[33]L. S. Cederbaum and W. Domcke, Adv. Chem. Phys. 36, 205 (1977).
[34]E. B. Wilson, J. C. Decius, and P. C. Cross, *Molecular Vibrations* (McGraw-Hill, New York, 1965).
[35]M. Born and K. Huang, *Dynamical Theory of Crystal Lattices* (Oxford U.P., London, 1954), Appendix VII.
[36]A. W. Weiss and M. Krauss, J. Chem. Phys. 52, 4363 (1970); M. Krauss and D. Neumann, Chem. Phys. Lett. 14, 26 (1972); J. Res. Nat. Bur. Stand. A77, 411 (1973).
[37]C. R. Claydon, G. A. Segal, and H. S. Taylor, J. Chem. Phys. 52, 3387 (1970).
[38]H. S. Taylor and J. K. Williams, J. Chem. Phys. 42, 4063 (1965).
[39]H. S. Taylor, G. V. Nazaroff, and A. Golebiewski, J. Chem. Phys. 45, 2872 (1966); I. Eliezer, H. S. Taylor, and J. K. Williams, J. Chem. Phys. 47, 2165 (1967).
[40]M. A. Morrison and N. F. Lane, Phys. Rev. A 12, 2361 (1975).
[41]P. W. Anderson, Phys. Rev. 124, 41 (1961).
[42]T. Moriya, in *Proceedings of the International School of Physics, "Enrico Fermi," Varenna, 1966* (Academic, New York, 1967), p. 206.
[43]D. M. Newns, Phys. Rev. 178, 1123 (1969); W. Brenig and K. Schönhammer, Z. Phys. 267, 201 (1974).
[44]E. L. Breig and C. C. Lin, J. Chem. Phys. 43, 3839 (1965); Y. Itikawa, Phys. Rev. A 3, 831 (1971).
[45]A. S. Davydov, in Ref. 29, Chaps. XII and XIV.
[46]F. J. Dyson, Phys. Rev. 75, 486 (1949).
[47]J. N. Bardsley, A. Herzenberg, and F. Mandl, Proc. Phys. Soc. Lond. 89, 321 (1966).
[48]M. Abramowitz and I. A. Stegun, *Handbook of Mathematical Functions* (Dover, New York, 1965).
[49]B. I. Schneider, Phys. Rev. A 14, 1923 (1976).
[50]L. S. Cederbaum and W. Domcke, Z. Phys. A227, 221 (1976).
[51]L. Mazeau, F. Gresteau, R. I. Hall, G. Joyez, and J. Reinhardt, J. Phys. B 6, 862 (1973).
[52]D. C. Tyte, in *Advances in Quantum Electronics*, Vol. I, edited by D. W. Goodwin (Academic, London, 1970), p. 129.
[53]M. J. W. Boness and J. B. Hasted, Phys. Lett. 21, 526 (1966).
[54]L. Sanche and G. J. Schulz, J. Chem. Phys. 58, 479 (1973).
[55]P. D. Burrow and L. Sanche, Phys. Rev. Lett. 28, 333 (1972).
[56]M. J. W. Boness and G. J. Schulz, Phys. Rev. Lett. 21, 1031 (1968).
[57]D. Danner, thesis (Physikalisches Institut der Universität Freiburg, Germany, 1970) (unpublished).
[58]D. Andrick and F. H. Read, J. Phys. B 4, 389 (1971).
[59]D. Andrick, D. Danner, and H. Erhardt, Phys. Lett. A29, 346 (1969).
[60]I. Suzuki, J. Mol. Spectrosc. 25, 479 (1968).
[61]J. C. Y. Chen, Phys. Lett. 8, 183 (1964); J. Chem. Phys. 40, 3513 (1964); 45, 2710 (1966).
[62]J. B. Hasted and A. M. Awan, J. Phys. B 2, 367 (1969).
[63]G. J. Schulz, Phys. Rev. 135, A988 (1964).
[64]M. Krauss and F. H. Mies, Phys. Rev. A 1, 1592 (1970).
[65]H. Ehrhardt and K. Willmann, Z. Phys. 204, 462 (1967).
[66]I. Özkan, S. Y. Chu, and L. Goodman, J. Chem. Phys. 63, 3195 (1975).
[67]A. D. McLean and M. Yoshimine, IBM J. Res. Develop. Suppl. (1967).
[68]W. von Niessen (private communication).
[69]D. J. Thouless, Nucl. Phys. 22, 78 (1961).